

Supplementary Files

MPS@BWO with High Adsorption Capacity for Efficient Photocatalytic Reduction of CO₂

Peng Chen ¹, Tao Du ^{1,2,*}, Yingnan Li ³, He Jia ⁴, Gemeng Cao ¹, Junxu Zhang ¹
and Yisong Wang ^{1,2,*}

Address:

1 State Environmental Protection Key Laboratory of Eco-Industry, Northeastern University, Shenyang 110819, China

2 Engineering Research Center of Frontier Technologies for Low-Carbon Steelmaking (Ministry of Education), Shenyang 110819, China

3 Liaoning Province Engineering Research Center for Technologies of Low-Carbon Steelmaking, Northeastern University, Shenyang 110819, China

4 Institute for Frontier Technologies of Low-Carbon Steelmaking, Northeastern University, Shenyang 110819, China

*** Corresponding author.**

Email: dut@smm.neu.edu.cn (Tao Du)

Email: wangys@smm.neu.edu.cn (Yisong Wang)

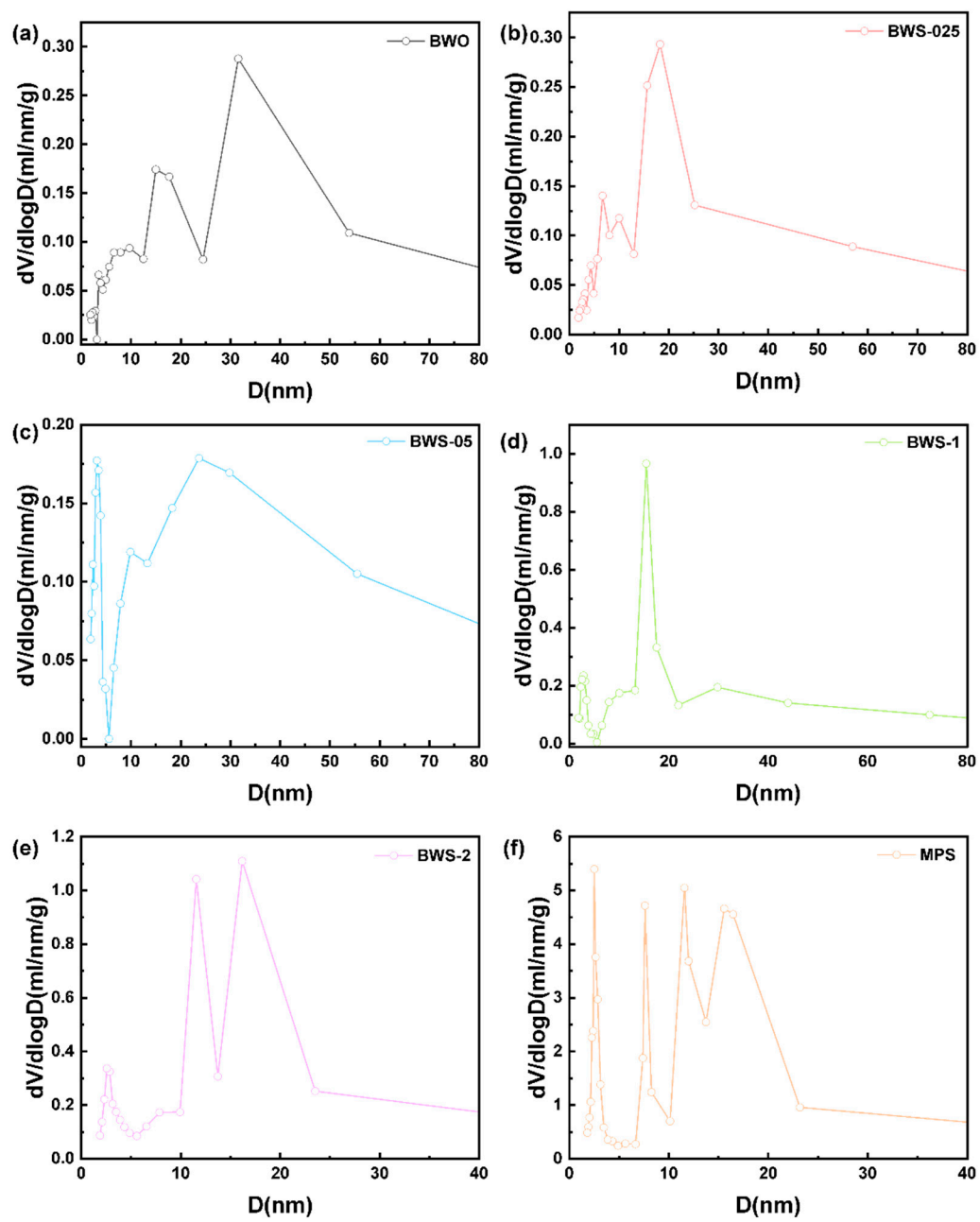


Figure S1 Pore structure of photocatalysts

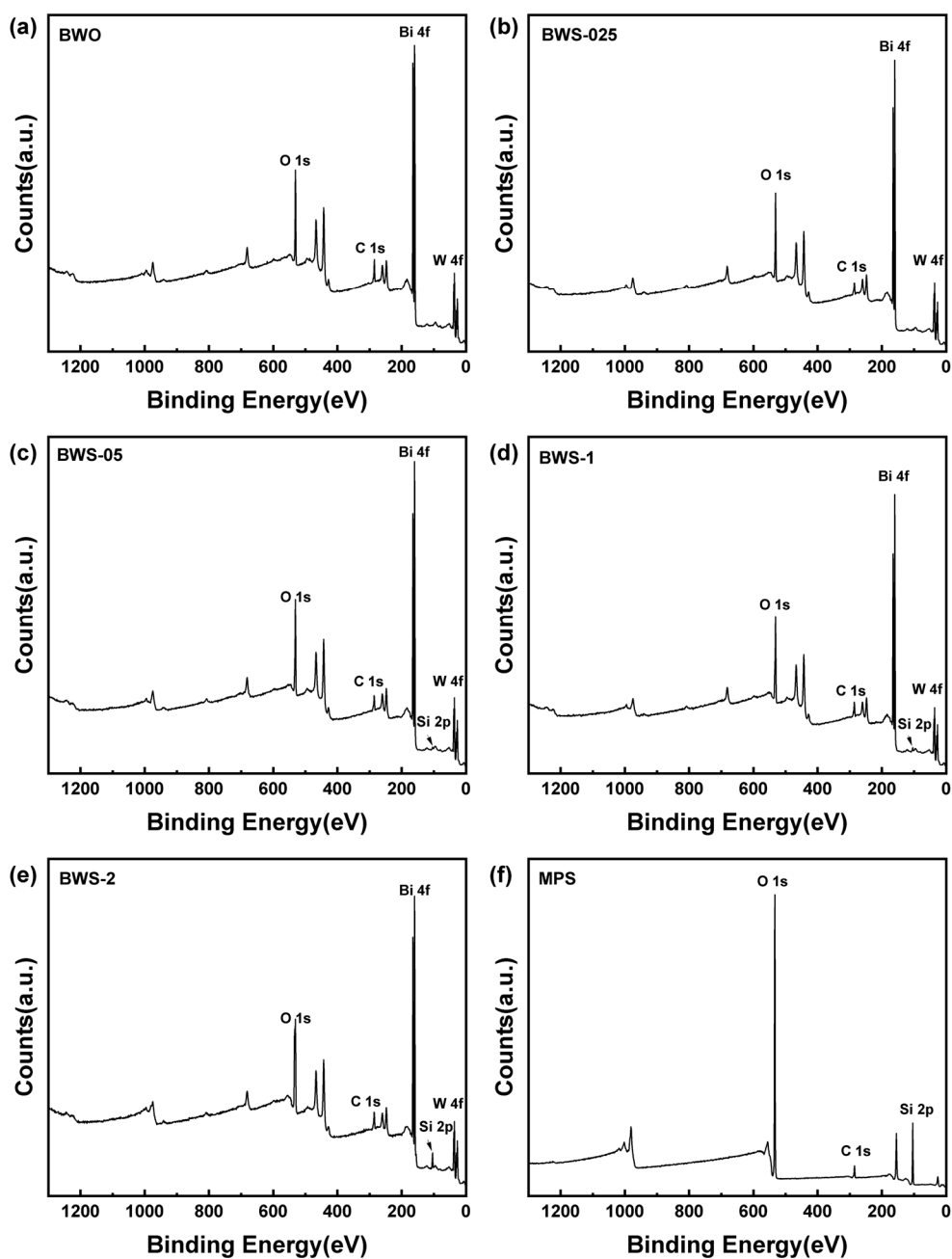


Figure S2 XPS survey spectra of photocatalysts



Figure S3 Results of GC analysis

The product corresponding to the peak appearing near 16 min is CO. Before calculating the CO yield, the reaction system was filled with 80 kPa CO₂, and an equal amount of standard gas was injected into the inlet every hour for detection. The functional relationship between the peak area and the CO content was established. In the photocatalytic reaction, the CO peak area of the product is compared with the data in the function to obtain the yield of CO. The peak appearing near 5-6 minutes is a fluctuation during system detection and has nothing to do with the result.

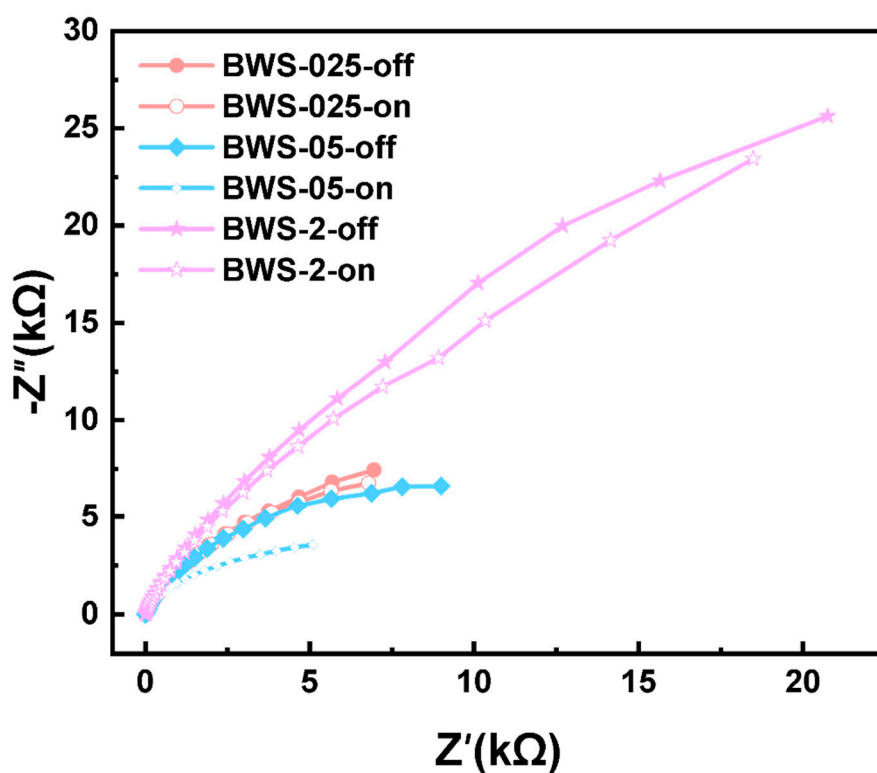


Figure S4 the Nyquist plot of BWS-025, BWS-05 and BWS-2

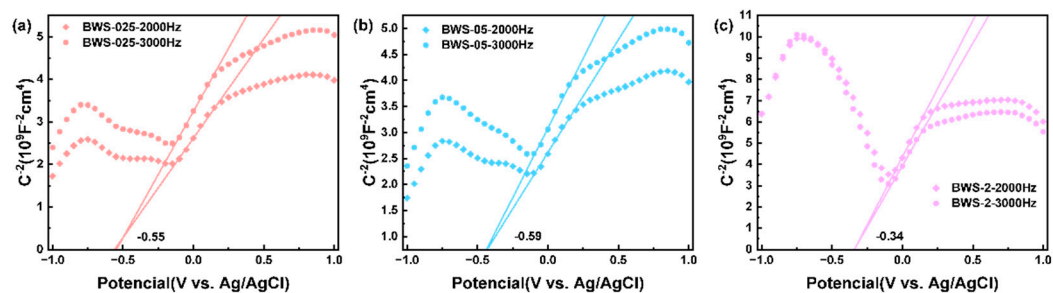


Figure S5 Mott-Schottky diagrams of (a) BWS-025, (b) BWS-05 and (c) BWS-2

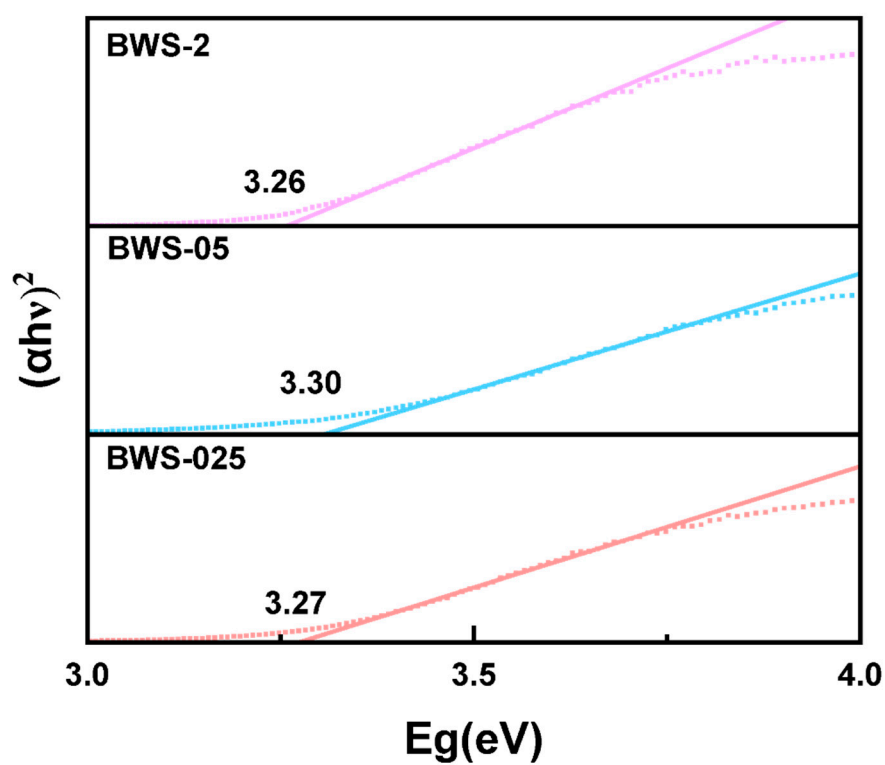


Figure S6 the bandgap of BWS-025, BWS-05 and BWS-2

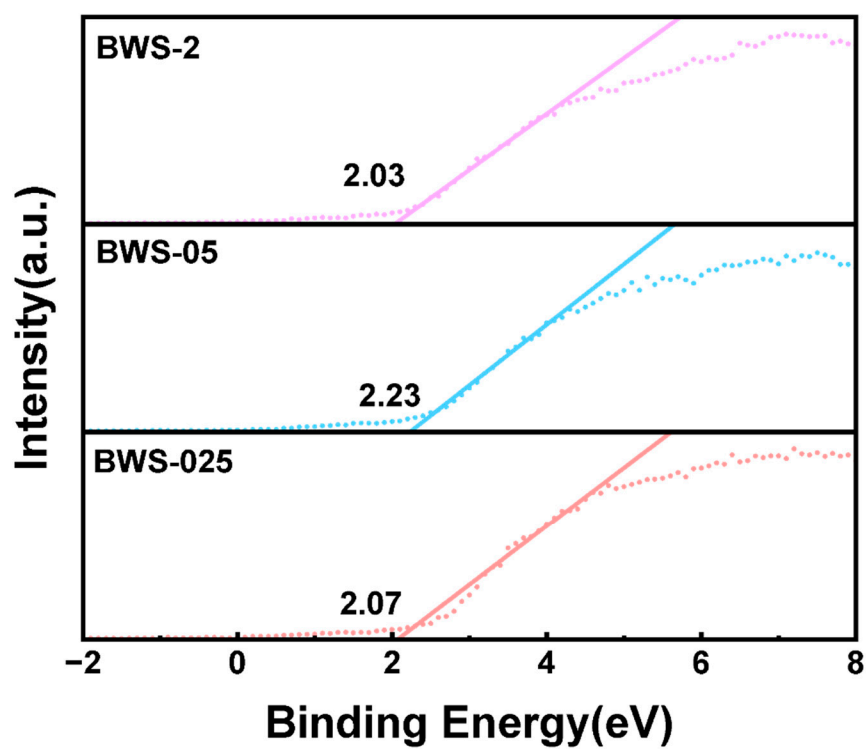


Figure S7 the VB-XPS spectra of BWS-025, BWS-05 and BWS-2

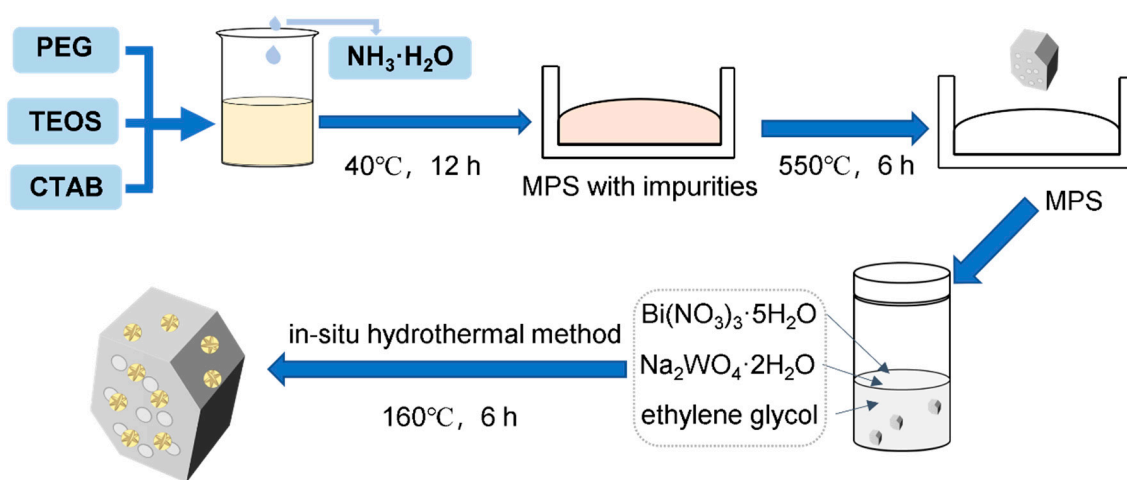


Figure S8 Scheme of the photocatalyst synthesis

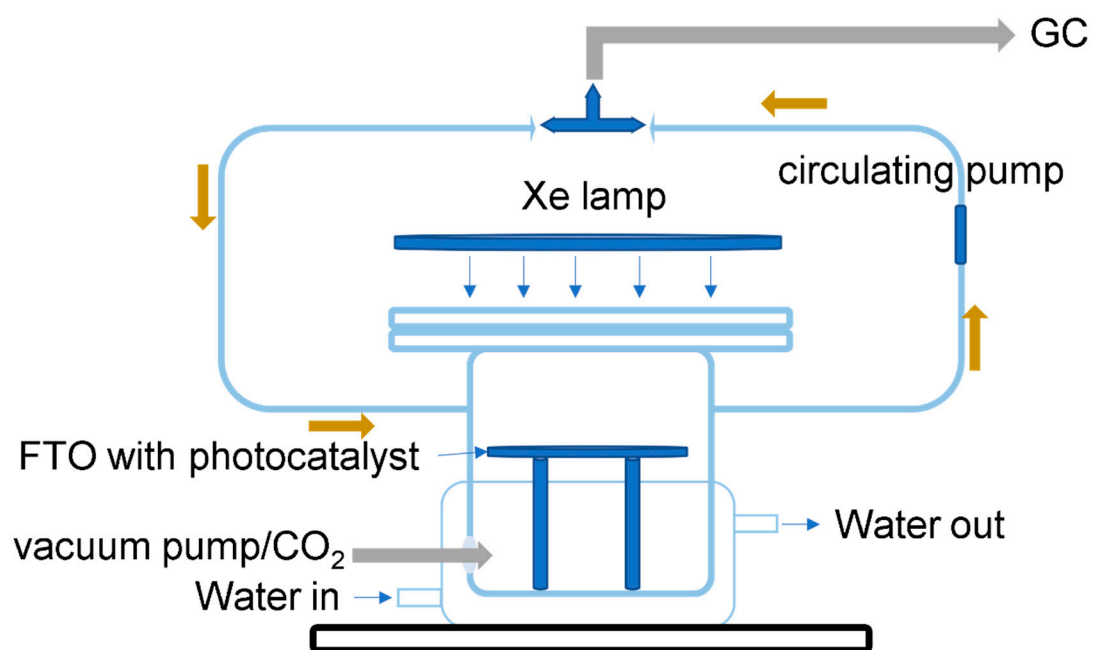


Figure S9 Scheme of the photocatalytic reduction

Table S1 Comparison of some materials on photocatalytic CO₂ reduction.

Photocatalyst	Light source	Reaction system	Yields ($\mu\text{mol} \cdot \text{g}^{-1} \cdot \text{h}^{-1}$)	Ref.
Bi ₂ WO ₆ /TiO ₂	UV–visible 250 W mercury vapor lamps	100 mg photocatalyst, 20 mL deionized water, 1 bar, 25 °C	CH ₄ : 2.37	[54]
Bi ₂ WO ₆ /C ₃ N ₅	300 W Xe lamp	50 mg catalyst, 100 mL water, 20 °C, high-purity CO ₂	CH ₄ : 1.976	[55]
g-C ₃ N ₄ /Bi ₂ WO ₆	300 W xenon lamp with a AM1.5 filter	3 mg photocatalyst, rhodamine B (RhB) (5 mL, 10 mg/L), high-purity CO ₂ , at atmospheric pressure, 6 °C	CO: 4.3 CH ₄ : 2.7	[56]
RuO ₂ /Bi ₂ WO ₆ PtO ₂ - Pt/Bi ₂ WO ₆	300 W xenon lamp equipped with 420 nm cut- off filter	50 mg photocatalyst, high purity of CO ₂ gas, ambient pressure, 1.0 mL deionized water	CO: 0.9719 CH ₄ :0.1249 CO: 0.9787 CH ₄ : 0.0646	[57]
Bi ₂ WO ₆ /BCDs	300 W Xe lamp with a 420 nm cut off filter	0.05 g photocatalyst, 90 mL H ₂ O, 10 mL TEOA, 25°C, CO ₂ (99.999 %)	CO: 1.82 CH ₄ : 0.55	[58]
Cs ₂ AgBiBr ₆ /Bi ₂ WO ₆	Xe lamp (300 W, 420 nm \leq $\lambda \leq$ 800 nm)	a mixture of EA (2 mL) and isopropanol (IPA, 0.2 mL) saturated with CO ₂ , 10 mg photocatalyst	CO: 1.925 CH ₄ : 0.4	[59]
hollow- hierarchical structured Bi ₂ WO ₆	300 W Xe lamp	10 mg catalysts, 5 mL DI water, high purity CO ₂ gas, room-temperature (25 °C)	CH ₄ : 2.6	[60]
MPS@Bi ₂ WO ₆	300W Xe lamp	20 mg photocatalysts, 5 mL H ₂ O, 80 kPa CO ₂	CO: 4.918	This work

References

54. Ahmadi, M.; Alavi, S.M.; Larimi, A. UV–Vis Light Responsive Bi₂WO₆ Nanosheet/TiO₂ Nanobelt Heterojunction Photo-Catalyst for CO₂ Reduction. *Catalysis Communications* **2023**, *179*, 106681.
55. Zhang, H.; Bian, H.; Wang, F.; Li, Y.; Zhu, L.; Xia, D. 2D/2D Bi₂WO₆/C₃N₅ S-Scheme Heterojunction for Highly Selective Production of CH₄ by Photocatalytic CO₂ Reduction under Visible Light. *Applied Catalysis A: General* **2024**, *686*, 119914.
56. Zhang, B.; Liu, Y.; Wang, D.; He, W.; Fang, X.; Zhao, C.; Pan, J.; Liu, D.; Liu, S.; Chen, T.; et al. Nanoengineering Construction of G-C₃N₄/Bi₂WO₆ S-Scheme Heterojunctions for Cooperative Enhanced Photocatalytic CO₂ Reduction and Pollutant Degradation. *Separation and Purification Technology* **2025**, *354*, 128893.
57. Jiang, H.; An, Q.; Zang, S. Ultrathin RuO₂/Bi₂WO₆ and PtO₂-Pt/Bi₂WO₆ Heterojunction Nanosheets toward Efficient Photocatalytic CO₂ Reduction under Visible Light Irradiation. *Journal of Environmental Chemical Engineering* **2023**, *11*, 110960.
58. Li, X.; Yu, Y.; Wang, Y.; Di, Y.; Liu, J.; Li, D.; Wang, Y.; Zhu, Z.; Liu, H.; Wei, M. Withered Magnolia-Derived BCDs onto 3D Flower-like Bi₂WO₆ for Efficient Photocatalytic TC Degradation and CO₂ Reduction. *Journal of Alloys and Compounds* **2023**, *965*, 171520.
59. Wang, J.; Cheng, H.; Wei, D.; Li, Z. Ultrasonic-Assisted Fabrication of Cs₂AgBiBr₆/Bi₂WO₆ S-Scheme Heterojunction for Photocatalytic CO₂ Reduction under Visible Light. *Chinese Journal of Catalysis* **2022**, *43*, 2606–2614.
60. Xiao, L.; Lin, R.; Wang, J.; Cui, C.; Wang, J.; Li, Z. A Novel Hollow-Hierarchical Structured Bi₂WO₆ with Enhanced Photocatalytic Activity for CO₂ Photoreduction. *Journal of Colloid and Interface Science* **2018**, *523*, 151–158.